Stem Cell Research 38 (2019) 101453

Contents lists available at ScienceDirect

Stem Cell Research

journal homepage: www.elsevier.com/locate/scr

Lab Resource: Multiple Cell Lines

The use of simultaneous reprogramming and gene correction to generate an osteogenesis imperfecta patient *COL1A1* c. 3936 G > T iPSC line and an isogenic control iPSC line

Sara Howden[a], Hani Hosseini Far[a,b], Ali Motazedian[a], Andrew G. Elefanty[a,b,c], Edouard G. Stanley[a,b,c], Shireen R. Lamandé[a,b], John F. Bateman[a,d,*]

[a] *Murdoch Children's Research Institute, Australia*
[b] *Department of Paediatrics, University of Melbourne, Australia*
[c] *Department of Anatomy and Developmental Biology, Monash University, Australia*
[d] *Department of Biochemistry and Molecular Biology, University of Melbourne, Australia*

A B S T R A C T

To develop a disease model for the human 'brittle bone' disease, osteogenesis imperfecta, we used a simultaneous reprogramming and CRISPR-Cas9 genome editing method to produce an iPSC line with the heterozygous patient mutation (*COL1A1* c. 3936 G > T) along with an isogenic gene-corrected control iPSC line. Both IPSC lines had a normal karyotype, expressed pluripotency markers and differentiated into cells representative of the three embryonic germ layers. This osteogenesis imperfecta mutant and isogenic iPSC control line will be of use in exploring disease mechanisms and therapeutic approaches *in vitro*.

Resource table.

Unique stem cell lines identifier	MCRIi018-A MCRIi018-B
Alternative names of stem cell lines	OI64-mutant (MCRIi018-A) OI64–control (MCRIi018-B)
Institution	Murdoch Children's Research Institute, Melbourne, Australia
Contact information of distributor	Professor John Bateman john.bateman@mcri.edu.au
Type of cell lines	iPSC
Origin	Human
Cell Source	Fibroblasts
Clonality	Clonal
Method of reprogramming	Episomal
Multiline rationale	Generate osteogenesis imperfecta patient iPSC along with isogenic control iPSC
Gene modification	Yes
Type of modification	Gene Correction
Associated disease	Osteogenesis imperfecta. OMIM #166210
Gene/locus	COL1A1/c.3936 G > T
Method of modification	CRISPR/Cas9
Name of transgene or resistance	N/A
Inducible/constitutive system	N/A
Date archived/stock date	October 2017
Cell line repository /bank	https://hpscreg.eu/cell-line/MCRIi018-A; https://hpscreg.eu/cell-line/MCRIi018-B
Ethical approval	RCH Human Research Ethics Committee HREC 33118A

Resource utility

This heterozygous OI64 iPSC line, paired with the gene-corrected isogenic control iPSC, will provide an *in vitro* human model system to explore osteogenesis imperfecta disease mechanisms and test new therapeutic strategies.

Resource details

The 'brittle-bone' disorder, osteogenesis imperfecta (OI), is commonly caused by heterozygous mutations in the genes for type I collagen, *COL1A1* and *COL1A2*. To develop an OI iPSC disease modelling system for disease mechanism and therapeutic studies, we generated an iPSC line from a patient with the lethal perinatal form of osteogenesis imperfecta, MCRIi018-A (OI64-mutant). The mutation was a heterozygous single base substitution in *COL1A1* exon 49 (c.3936 G > T) leading to a p.Trp1312Cys substitution (https://oi.gene.le.ac.uk/ DB-ID COL1A1_00271; PMID: 7721766) in the C-propeptide domain of the type I procollagen proα1(I) chain, disrupting procollagen trimerization. Using a simultaneous reprogramming and CRISPR/Cas9 gene correction approach (Howden et al., 2018) we also generated an isogenic

* Corresponding author at: Murdoch Children's Research Institute, Australia.
E-mail address: john.bateman@mcri.edu.au (J.F. Bateman).

https://doi.org/10.1016/j.scr.2019.101453
Received 17 March 2019; Received in revised form 23 April 2019; Accepted 29 April 2019
Available online 04 May 2019

Table 1
Summary of lines.

iPSC line names	Abbreviation in figures	Gender	Age	Ethnicity	Genotype of locus	Disease
MCRIi018-A	OI64-mutant	Female	Newborn	Caucasian	*COL1A1*	Osteogenesis Imperfecta OMIM # 166210
MCRIi018-B	OI64–control	Female	Newborn	Caucasian	*COL1A1*	Osteogenesis Imperfecta (gene corrected)

control line, MCRIi018-B (OI64-control) (Table 1).

Episomal reprogramming plasmids, *in vitro* transcribed mRNA encoding SpCas9, a plasmid encoding a *COL1A1*-specific sgRNA and an oligodeoxynucleotide (ODN) for homology directed repair (HDR) of the patient-specific mutation were co-transfected into OI64 patient fibroblasts. Individual iPSC colonies were isolated, expanded and screened by PCR using a primer that overlaps the 3 bp synonymous changes incorporated in the ODN used for HDR repair (Fig. 1A). Heterozygous mutant and gene-corrected iPSCs were confirmed by Sanger sequencing (Fig. 1A). The gene-corrected iPSC clone had undergone biallelic HDR as indicated by homozygous insertion of the three bp synonymous change (p.Ser1329Ser), and the single synonymous change (p.Ala1308Ala) that had been incorporated into the repair ODN to facilitate screening (Fig. 1A). The colonies of OI64 and gene-corrected control, OI64-control, had normal stem cell morphology with well-defined boundaries and an increased nuclear-cytoplasmic ratio (Fig. 1B). Flow cytometry showed that 92% and 98% of the cell population of OI64-mutant and OI64-control, respectively, expressed pluripotency cell surface markers CD9 and TRA1-81 (Fig. 1B) and immunofluorescent staining confirmed the co-expression of nuclear pluripotency transcription factors, OCT4 and NANOG (Fig. 1C, Table 2).

Genome SNP array analysis of both lines confirmed no aneuploidies or large deletions or insertions and > 99.9% identity between MCRIi018-A and MCRIi018-B (Table 3 and Supplementary Fig. 1). It should be noted that the SNP analysis does not preclude the presence of balanced translocations.

The ability of both iPSC lines to differentiate into derivatives of the three germ layers was confirmed. Directed differentiation to definitive endoderm (Loh et al., 2014) induced co-expression of the endoderm markers SOX17 (Fig. 1D), CXCR4 and EpCAM (Fig. 1D). Neuroectoderm was demonstrated by co-expression of Nestin and PAX6 (Fig. 1E) after directed differentiation (Tchieu et al., 2017). CD45 expression (Fig. 1F) indicated that both OI64mutant and OI64control iPSC lines could differentiate into blood, a mesoderm derivative (Ng et al., 2016).

Both iPSC lines were confirmed to be free from mycoplasma contamination (Supplementary Fig. 2).

Materials and methods

Cell culture

Fibroblasts were cultured in DMEM (Thermo Fisher Scientific) supplemented with 15% fetal bovine serum (HyClone) at 37 °C, 5% CO_2, and 5% O_2. All iPSC lines were maintained on Matrigel-coated plates (Corning) and expanded in Essential 8 (E8) medium (Thermo Fisher Scientific) with daily media changes and passaged (1:3–1:6 split) every 3–4 days with 0.5 mM EDTA in PBS as previously described (Chen et al., 2011).

Reprogramming and Cas9-mediated gene editing

The method for simultaneous reprogramming and gene correction is described in detail by Howden et al. (Howden et al., 2018). Cells were transfected using the Neon Transfection System (Thermo Fisher Scientific). Cells were harvested with TrypLE (Thermo Fisher Scientific) 2 days after passaging and resuspended in Buffer R at a final concentration of 1–3 × 10^7 cells/ml. One hundred microliters of the cell suspension was added to a tube containing plasmids required for both reprogramming and gene targeting as well as mRNA encoding SpCas9 (Table 3). *In vitro* transcribed mRNA encoding a truncated version of the EBNA1 protein was also included to enhance nuclear uptake of the reprogramming plasmids. Electroporation was performed in 100 µl tips using the following conditions: 1400 V, 20 ms, two pulses. Following electroporation, cells were plated on a single 10 cm Matrigel-coated plate (Corning) and maintained in fibroblast medium for 4 days post transfection, then switched to E7 medium (Thermo Fisher Scientific; E8

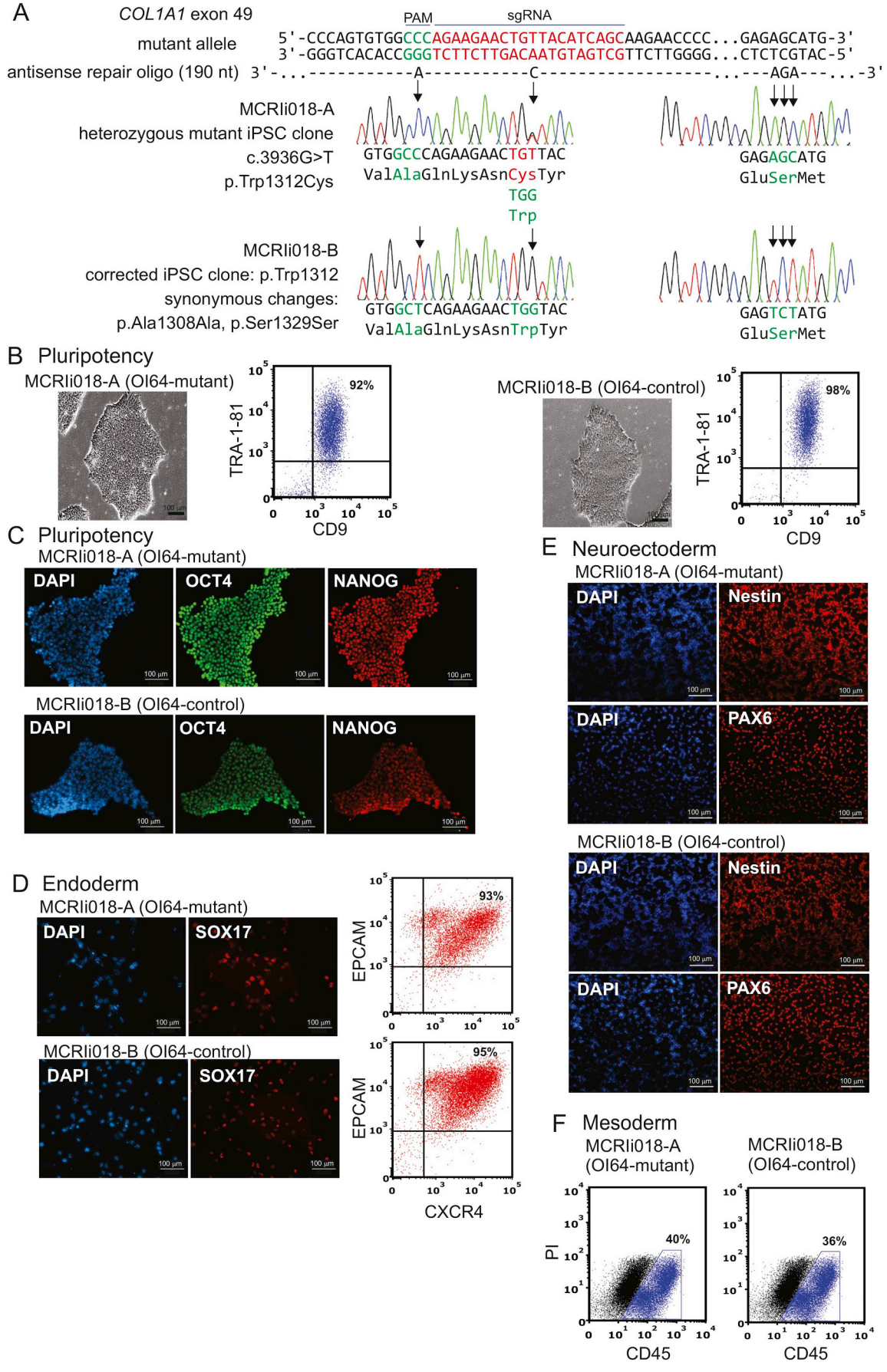

Fig. 1. Cellular and molecular characterization.

Table 2
Characterization and validation.

Classification	Test	Result	Data
Morphology	Photography	Normal	Fig. 1 panel B
Phenotype	Qualitative analysis (Immunofluorescence)	OCT4 and NANOG Both lines positive	Fig. 1 panel B
	Quantitative analysis (Flow cytometry)	CD9 and TRA1–81 MCRIi018-A 92% MCRIi018-B 98%	Fig. 1 panel C
Genotype	SNP array (resolution 0.5 Mb)	46XX Both lines. No aneuploidies were detected	Supplementary Fig. 1
Identity	Genetic analysis	SNPduo of SNParrays to compare iPSC mutant and gene edited control iPSC clones. Identical genotypes (> 99.9%) for the entire genome, indicating the lines are from the same individual	Report presented in Supplementary Fig. 1
Mutation analysis	Sequencing	Heterozygous OI mutation confirmed in MCRIi018A -*COL1A1* (c.3936 G > T). MCRIi018-B homozygous *COL1A1* (c.3936 G)	Fig. 1 panel A
Microbiology and virology	Mycoplasma	Mycoplasma testing by PCR. Both lines negative	Report presented in Supplementary Fig. 2
Differentiation potential	Directed differentiation (Immunofluorescence and Flow cytometry)	Endoderm: SOX17, CXCR4 and EpCAM. Ectoderm: Nestin, and PAX6 Mesoderm (Blood mesoderm); CD45	Fig. 1 panels D,E,F
Donor screening (OPTIONAL)	HIV 1 + 2 Hepatitis B, Hepatitis C	N/A	N/A
Genotype additional info (OPTIONAL)	Blood group genotyping	N/A	N/A
	HLA tissue typing	N/A	N/A

medium without transforming growth factor β) supplemented with 100 mM sodium butyrate and changed every second day as described previously (Chen et al., 2011). Sodium butyrate was removed from the medium after the appearance of the first iPSC colonies at around day 14. Targeted corrected clones and mutant uncorrected clones were identified by allele-specific PCR (Table 3) and by sequencing (Fig. 1A).

PCR

For PCR screening of mutant and gene corrected iPSC clones, gDNA was extracted using a DNAeasy Blood and Tissue Kit (Qiagen) according to the manufacturer's instructions. PCR was performed using GoTaq Green Mastermix (Promega) with the primer sets specified in Table 3 using an Applied Biosystems (Veriti) 96-well thermocycler. PCR conditions were 95 °C for 3 min, followed by 35 cycles of 95 °C for 18 s, 55 °C for 18 s, 72 °C for 40 s then 72 °C for 5 min. PCR products were analysed by agarose gel electrophoresis.

Immunocytochemistry

Cells in 12 well culture plates or on glass slides were fixed in 4% paraformaldehyde for 20 min at room temperature, followed by permeabilization with solution containing 0.05% Triton X-100 in PBS for 10 min at 4 °C. The cells were then incubated in blocking solution consisting of 3% bovine serum albumin in 0.1% PBST (PBS + Tween-20) for 30 min at room temperature and stained overnight at 4 °C with primary antibodies diluted in 1% bovine serum albumin in 0.1% PBST. Secondary antibodies, diluted in 1% bovine serum albumin in 0.1% PBST, were applied for 1 h at room temperature. Antibodies are listed in Table 3. Cells were incubated with DAPI (1 μg/ml) to counterstain nuclei prior to visualisation by fluorescent microscopy (Olympus IX70).

Flow cytometry

Cells were dissociated with TrypLE (Thermo Fisher Scientific) for 3 min at 37 °C. Harvested iPSCs were incubated with directly conjugated antibodies (Table 3) diluted in PBS containing 3% fetal bovine serum (GE Healthcare) for 20 min at 4 °C. Isotype controls were used for gating (Table 3). Propidium iodide (Sigma) was used to identify dead cells. Samples were analysed using a BD LSRII (BD Biosciences) using BD FACSDiva software.

Differentiation

iPSCs were differentiated in monolayer culture into definitive endoderm (Loh et al., 2014) and analysed by flow cytometry and immunocytochemistry after 4 days. Ectoderm potential was assessed by differentiation to neuroectoderm for 12 days (Tchieu et al., 2017) and immunocytochemical analysis. Mesodermal differentiation potential was confirmed by directed differentiation to blood mesoderm for 22 days (Ng et al., 2016) and analysis by flow cytometry.

SNP analysis

Cell pellets (at passage 4–6) were provided to the Victorian Clinical Genetics Service (Murdoch Children's Research Institute, Melbourne, Australia) and genomic DNA was analysed using an Infinium CoreExome-24 v1.1 SNP array (Illumina). Mutant and gene-corrected iPSC lines were compared using SNPduo (http://pevsnerlab.kennedykrieger.org/SNPduo/).

Mycoplasma detection

Absence of mycoplasma contamination was confirmed by PCR by the commercial service provider Cerberus Sciences (Adelaide, Australia).

Table 3
Reagents details.

Reprogramming and genome editing plasmids		
	Plasmid	Company Cat #
Reprogramming	pEP4 E02S ET2K	Addgene plasmid #20927
Reprogramming	pEP4 E02S EN2L	Addgene plasmid #20922
Reprogramming	pEP4 E02S EM2K	Addgene plasmid #20923
Reprogramming	pSimple-miR302/367	Addgene plasmid #98748
Genome editing	pSMART-sgRNA(Sp)	Addgene plasmid #80427
Reprogramming	pSP6-EBNA$^{2A + DBD}$	Addgene plasmid #98749
Genome editing	pDNR-SpCas9-Gem	Addgene plasmid #98749

Antibodies used for immunocytochemistry/flow cytometry			
	Antibody	Dilution	Company Cat # and RRID
Pluripotency marker	Mouse anti-CD9 Monoclonal Antibody, FITC conjugated, Clone M-L13	1/20	BD Biosciences Cat# 555371, RRID: AB_395773
Pluripotency marker	Alex Fluor 647 anti-human TRA-1-81 antibody	1/50	BioLegend Cat# 330706, RRID: AB_1089242
Pluripotency marker	Mouse anti-Human NANOG purified, eBioscience	1/200	ThermoFisher Scientific Cat# 14–5769-80, RRID: AB_467573
Pluripotency marker	Oct-4A (C30A3) Rabbit mAb	1/400	Cell Signaling Technology Cat# 2840, RRID: AB_2167691
Differentiation marker	PE/Cy7 conjugated anti-human CD184 (CXCR4) antibody	1/40	BioLegend Cat# 306514, RRID: AB_2089651
Differentiation marker	PE/Cy7 anti-human CD326 (EPCAM) antibody	1/100	BioLegend Cat# 324222, RRID: AB_2561506
Differentiation marker	BV 421 conjugated anti-human CD326 (EPCAM) antibody	1/50	BioLegend Cat# 324220, RRID: AB_2563847
Differentiation marker	BV 421 anti-human CD45 antibody	1/40	BioLegend Cat# 304032, RRID: AB_2561357
Differentiation marker	Goat anti-SOX17	1/500	R&D Systems Cat# AF1924, RRID: AB_355060
Differentiation marker	Mouse Anti-Nestin Antibody, clone 10C2	1/300	Merck Cat# MAB5326, RRID: AB_2251134
Differentiation marker	Mouse Human/Mouse/Rat SOX2 Antibody	1/300	R&D Systems Cat# MAB2018, RRID: AB_358009
Differentiation marker	Mouse anti-PAX6	1/300	DSHB Cat# Pax6, RRID: AB_2315070
Secondary antibody	Donkey anti-Mouse IgG (H&L) Highly Cross-Adsorbed Secondary Antibody, Alexa Fluor 594	1/1000	ThermoFisher Scientific Cat# A21203, RRID: AB_2535789
Secondary antibody	Donkey anti-Goat IgG (H&L) Cross-Adsorbed Secondary Antibody, Alexa Fluor 647	1/1000	ThermoFisher Scientific Cat# A21447, RRID: AB_2535864
Secondary antibody	Goat anti-Rabbit IgG (H&L) Cross-Adsorbed Secondary Antibody, Alexa Fluor 488	1/1000	ThermoFisher Scientific Cat# A11008, RRID: AB_143165
Isotype control	FITC Mouse IgG1κ	1/100	BD Biosciences Cat# 555748, RRID: AB_396090
Isotype control	APC Mouse IgG1κ	1/100	BD Biosciences Cat# 555751, RRID: AB_398613
Isotype control	Brilliant Violet 421 Mouse IgG2bκ	1/100	BioLegend Cat# 400341, RRID: AB_10898160
Isotype control	PE/Cy7 Mouse IgG1κ	1/100	BioLegend Cat# 400126, RRID: AB_326448

Primers	
Target Forward/Reverse primer (5′-3′)	
COL1A1-OI64-sgRNA	
COL1A1 exon 49	
AGAAGAACTGGTACATCAGC/GCTGATGTACCAGTTCTTCT	
Mutant allele specific PCR	
COL1A1 exon 48–49	
530 bp	
CCAGCCACCTCAAGAGAAGG/GGAATCCATCGGTCATGCTC	
Edited allele specific PCR	
COL1A1 exon 48–49	
530 bp	
CCAGCCACCTCAAGAGAAGG/CTGGAATCCATCGGTCATAGA	
PCR and sequencing across edited region	
COL1A1 exon 48-intron 49	
539 bp	
CCAGCCACCTCAAGAGAAGG/CACGCACCTGGAATCCATCG	
ODN for HDR	
Overlaps patient mutation	
ACTGGCTCTGAGGTCCAGCTCACGCACCTGGAATCCATCGGTCATAGACTCGCCGAACCAGACATGCCTCTTGTCCTTGGGGTTCTTGCTGATGTAC CAGTTCTTCTGAGCCACACTGGGCTGAGTGGGGTACACGCAGGTCTCACCAGTCTCCATGTTGCAGAAGACTTTGATGGCATCCAGGTTGCAG	

Acknowledgements

This study was funded by an Australian National Health & Medical Research Council project grant (GNT1146952), the Victorian Government's Operational Infrastructure Support Program, Melbourne International Research Scholarship (HHF), Melbourne International Fee Remission Scholarship and Murdoch Children's Research Institute PhD Top Up Scholarship.

Appendix A. Supplementary data

Supplementary data to this article can be found online at https://doi.org/10.1016/j.scr.2019.101453.

References

Chen, G., Gulbranson, D.R., Hou, Z., Bolin, J.M., Ruotti, V., Probasco, M.D., Smuga-Otto, K., Howden, S.E., Diol, N.R., Propson, N.E., Wagner, R., Lee, G.O., Antosiewicz-

Bourget, J., Teng, J.M., Thomson, J.A., 2011. Chemically defined conditions for human iPSC derivation and culture. Nat. Methods 8, 424–429.
Howden, S.E., Thomson, J.A., Little, M.H., 2018. Simultaneous reprogramming and gene editing of human fibroblasts. Nat. Protoc. 13, 875–898.
Loh, K.M., Ang, L.T., Zhang, J., Kumar, V., Ang, J., Auyeong, J.Q., Lee, K.L., Choo, S.H., Lim, C.Y., Nichane, M., Tan, J., Noghabi, M.S., Azzola, L., Ng, E.S., Durruthy-Durruthy, J., Sebastiano, V., Poellinger, L., Elefanty, A.G., Stanley, E.G., Chen, Q., Prabhakar, S., Weissman, I.L., Lim, B., 2014. Efficient endoderm induction from human pluripotent stem cells by logically directing signals controlling lineage bifurcations. Cell Stem Cell 14, 237–252.
Ng, E.S., Azzola, L., Bruveris, F.F., Calvanese, V., Phipson, B., Vlahos, K., Hirst, C., Jokubaitis, V.J., Yu, Q.C., Maksimovic, J., Liebscher, S., Januar, V., Zhang, Z., Williams, B., Conscience, A., Durnall, J., Jackson, S., Costa, M., Elliott, D., Haylock, D.N., Nilsson, S.K., Saffery, R., Schenke-Layland, K., Oshlack, A., Mikkola, H.K., Stanley, E.G., Elefanty, A.G., 2016. Differentiation of human embryonic stem cells to HOXA(+) hemogenic vasculature that resembles the aorta-gonad-mesonephros. Nat. Biotechnol. 34, 1168–1179.
Tchieu, J., Zimmer, B., Fattahi, F., Amin, S., Zeltner, N., Chen, S., Studer, L., 2017. A modular platform for differentiation of human PSCs into all major ectodermal lineages. Cell Stem Cell 21 (399–410), e397.